JOURNAL OF BIOMOLECULAR STRUCTURE AND DYNAMICS
https://doi.org/10.1080/07391102.2020.1818623

Phthalocyanine complexes with (4-isopropylbenzyl)oxy substituents: preparation and evaluation of anti-carbonic anhydrase, anticholinesterase enzymes and molecular docking studies

Emre Güzel[a], Ümit M. Koçyiğit[b], Parham Taslimi[c], İlhami Gülçin[d], Sultan Erkan[e], Mehmet Nebioğlu[f], Barış S. Arslan[f] and İlkay Şişman[f]

[a]Department of Fundamental Sciences, Sakarya University of Applied Sciences, Sakarya, Turkey; [b]Department of Basic Pharmaceutical Sciences, Cumhuriyet University, Sivas, Turkey; [c]Department of Biotechnology, Bartın University, Bartın, Turkey; [d]Department of Chemistry, Atatürk University, Erzurum, Turkey; [e]Department of Chemistry and Chemical Processing Technologies, Yıldızeli Vocational School, Cumhuriyet University, Sivas, Turkey; [f]Department of Chemistry, Sakarya University, Sakarya, Turkey

Communicated by Ramaswamy H. Sarma

ABSTRACT

In this study, the preparation, aggregation behavior and investigation of carbonic anhydrase and cholinesterase enzyme inhibition features of non-peripherally (4-isopropylbenzyl)oxy-substituted phthalocyanines (**4–6**) are reported for the first time. The chemical structures of these new phthalocyanines were elucidated by UV-Vis (ultraviolet-visible), FT-IR (Fourier transform infrared spectrometry), NMR (nuclear magnetic resonance) and MALDI-TOF (matrix-assisted laser desorption/ionization time-of-flight) mass spectrometry. The substitution of 4-isopropylbenzyl)oxy groups benefits a remarkable solubility and redshift of the phthalocyanines Q-band. Also, these complexes were tested against some enzymes such as butyrylcholinesterase enzyme, human carbonic anhydrase I and II isoforms and acetylcholinesterase enzyme. The phthalocyanine complexes showed Ki values of in the range of 478.13 ± 57.25–887.25 ± 101.20 μM against hCA I, 525.16 ± 45.87–921.14 ± 81.25 μM against hCA II, 68.33 ± 9.13–201.15 ± 35.86 μM against AChE and 86.25 ± 13.65–237.54 ± 24.7 μM against BChE. Molecular docking studies were performed to investigate the binding modes and interaction energies of the (**2–6**) complexes with the hCA I (PDB ID:1BMZ), hCA II (PDB ID:2ABE), AChE (PDB ID:4EY6) and BChE (PDB ID:2PM8).

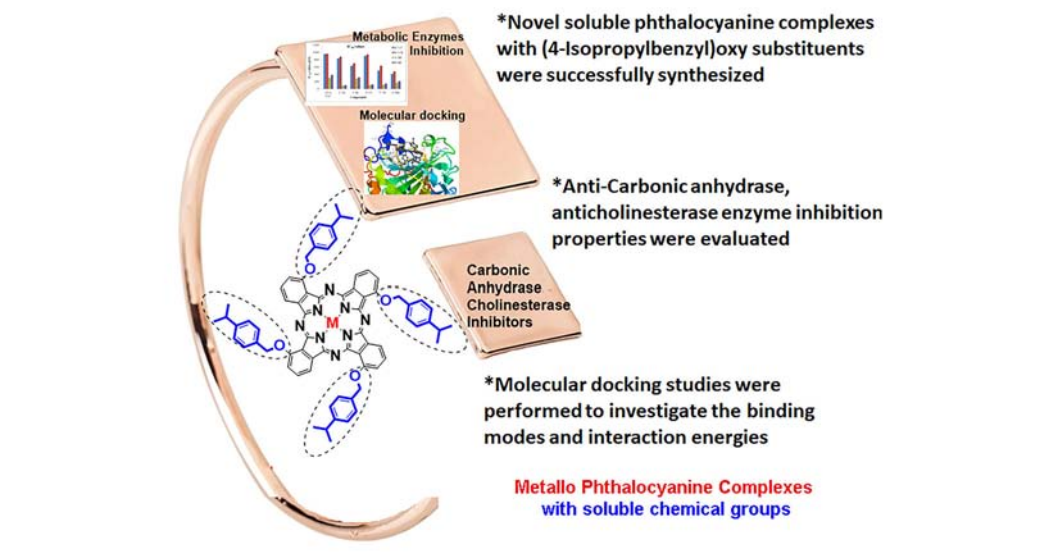

ARTICLE HISTORY
Received 13 May 2020
Accepted 28 August 2020

KEYWORDS
Phthalocyanine; carbonic anhydrase; cholinesterase; enzyme inhibition; molecular docking

CONTACT Emre Güzel eguzel@subu.edu.tr Department of Fundamental Sciences, Sakarya University of Applied Science, Sakarya 54050, Turkey; Ümit M. Koçyiğit ukocyigit@cumhuriyet.edu.tr Department of Basic Pharmaceutical Sciences, Cumhuriyet University, Sivas 58140, Turkey

Supplemental data for this article can be accessed online at https://doi.org/10.1080/07391102.2020.1818623.

Introduction

Phthalocyanines (Pcs), an important family of porphyrinoid complexes, have many applications such as gas sensors (Çimen et al., 2014), solar cells (Yıldız et al., 2019), liquid crystals phases (Chino et al., 2017; Korkut et al., 2017), electrochromic materials (Güzel, Orman, et al., 2019) and photosensitizer (Atilla et al., 2007; Güzel, 2019; Güzel et al., 2013; Sobotta et al., 2019; van de Winckel et al., 2017; Wierzchowski et al., 2020) in photodynamic therapy (PDT). Soluble functional chemical groups that can be substituted to the phthalocyanine ring, the interaction between the rings is reduced and the complexes can be highly dissolved in organic or aqueous solvents. Also, in this way, the wavelength of the absorption band of the phthalocyanine complexes can be adjusted. The introduction of 4-isopropylbenzyl)oxy to the non-peripheral positions of the complexes eliminates the solubility problems of these phthalocyanines and also contributes absorption at longer wavelengths when compared to unsubstituted phthalocyanines (Gürek & Bekaroğ lu, 1994; Güzel, Atmaca, et al., 2017; Önal et al., 2018; Ozoemena & Nyokong, 2002). So, these phthalocyanines are beneficial to optoelectronic, near IR devices and biological applications.

Carbonic anhydrase (CA) isoenzymes are metalloenzymes that catalyze a very easy reaction: the hydration of CO_2 to bicarbonate and H^+ (Mamedova et al., 2019; Taslimi et al., 2019). This key reaction plays a significant role in more pathological and physiological mechanisms associated with ion transport, pH control and fluid secretion (Erdemir et al., 2019). Their inhibition of these isoenzymes is the main goal correlated with the treatment of diverse diseases like obesity, glaucoma and epilepsy. More recently, CA inhibition was validated as a novel approach to fighting metastases and tumors (Boztas et al., 2019; Erdemir et al., 2019; Turkan et al., 2019a, 2019b).

The acetylcholine (ACh) molecule in the brain can be hydrolyzed by two kinds of cholinesterases including acetylcholinesterase (AChE) and butyrylcholinesterase (BChE) (El-Sayed et al., 2019; Genç Bilgiçli et al., 2019). AChE enzyme is more active than BChE enzyme and counting for approximately 80% ACh hydrolysis. Indeed, the inhibition act of AChE enzyme provides an impressive approach for the treatment of Alzheimer's disease (AD). Also, four AChE inhibitors (AChEIs) like donepezil, tacrine, galantamine and rivastigmine compounds have been approved by the FDA to improve cognitive functions and memorial of AD patients in the clinic. AChE enzyme is a protein involved in the termination of impulse transmission via rapid hydrolysis of the important neurotransmitter ACh, an advanced reduction of which had a main role in the pathogenesis of AD (Genç Bilgiçli et al., 2019; Turkan et al., 2019a, 2019b). Various drugs utilized in the therapy of AD are based on the established cholinergic hypothesis, where the objective is to raise the concentration of ACh molecule in the synaptic cleft by reducing of cholinesterase activity (Bursal et al., 2019; Turkan et al., 2019a, 2019b).

In this study, to investigate some metabolic enzymes inhibition properties, non-peripherally 4-isopropylbenzyl)oxy group containing phthalocyanines have been prepared. The synthesized phthalocyanine complexes showed good solubility and also recorded as anticholinergic and antiepileptic potentials. Besides, we investigate the activity with the mentioned metabolic enzymes of studied complexes by molecular docking studies.

Materials and methods

Instruments and chemicals

Shimadzu UV 2600 spectrophotometer system was used for UV-Vis studies. Infrared spectra were performed on a PerkinElmer FT-IR spectrophotometer. NMR spectra were performed on a Bruker 300 MHz spectrometer. The clusters of peaks that corresponded to the calculated isotope composition of the molecular ion were observed by MALDI-TOF mass spectrometry (Bruker). 2,5-dihydroxybenzoic acid (DHB) was used as matrix for MALDI-TOF mass spectrometry. The elemental analysis was performed on CHNS-932 (LECO). All starting materials and solvents were purchased from Merck and Aldrich Chemical Company. Silica gel (200–400 mesh, F254, Kieselgel 60, Merck) was utilized in the purification of molecules by column chromatography assay. 3-((4-isopropylbenzyl)oxy)phthalonitrile (**1**) and its soluble zinc and indium phthalocyanine derivatives (**2** and **3**) were prepared according to the reported method (Güzel, Arslan, et al., 2019).

General procedure for the synthesis of the phthalocyanines (2–6)

A mixture of 3-((4-isopropylbenzyl)oxy)phthalonitrile (1) (0.100 g, 0.36 mmol), anhydrous $ZnCl_2$, $InCl_3$, $CuCl_2$, $CoCl_2$, $CuCl_2$, $MnCl_3$ ~ (0.030 g, excess) in hexanol and 1,8-diazabicyclo[5.4.0]undec-7-ene (DBU, 0.05 mL) were heated to reflux temperature in sealed tube under an argon atmosphere for 16 h. After completion of the reaction, the resulting green mixture was cooled to room temperature. The crude products were precipitated by methanol–water, filtered off and then washed with the methanol–water mixture. The crude products were further purified by column chromatography using a mixture of THF:EtOH (10:1 v/v) as an eluent. Obtained Pcs **2–6** were highly soluble in ethylacetate, CH_2Cl_2, $CHCl_3$, DMF and DMSO.

Yield of **2**: 42 mg (40.1%). M.p. > 200 °C. FT-IR (υ_{max}/cm^{-1}): 3054 (m, Ar. C-H), 2957 (s, Aliph. C-H), 1590 (m, Ar. -C = C), 1487 (m, Aliph. C-H), 1334 (w, Ar.–C-N), 1271 (s, -R-O-Ar). ^{1}H NMR (300 MHz, $CDCl_3$) δ 7.56–7.48 (m, 4H), 7.45–7.05 (m, 24H), 5.55–5.46 (m, 8H), 3.09–2.94 (m, 4H), 1.30–1.24 (m, 24H). UV-Vis λ_{max} (nm) THF: 705, 633, 377. Anal. Calc. For $C_{72}H_{64}N_8O_4Zn$: C, 73.87; H, 5.51; N, 9.57; O, 5.47; Zn, 5.58; Found: C, 73.18; H, 5.34; N, 9.68. MS (MALDI-TOF): *m/z* 1169.75 $[M + H]^+$.

Yield of **3**: 34 mg (32.1%). M.p. > 200 °C. FT-IR (υ_{max}/cm^{-1}): 3057 (m, Ar. C-H), 2957s, Aliph. C-H), 1587 (m, Ar. -C = C), 1487 (m, Aliph. C-H), 1334 (w, Ar.–C-N), 1271 (s, -R-O-Ar). ^{1}H NMR (300 MHz, $CDCl_3$) δ 7.80–7.59 (m, 4H), 7.36–7.03 (m, 24H), 5.49–5.41 (m, 8H), 2.92–2.79 (m, 4H), 1.21–1.16 (m, 24H). UV-Vis λ_{max} (nm) THF: 721, 647, 366. Anal. Calc. For $C_{72}H_{64}ClInN_8O_4$: C, 68.87; H, 5.14; Cl, 2.82; In, 9.14; N, 8.92; O,

5.10. Found: C, 68.16; H, 5.02; N, 8.46. MS (MALDI-TOF): *m/z* 1219.98 $[M\text{-}Cl + H]^+$.

Yield of **4**: 49 mg (46.8%). M.p. > 200 °C. FT-IR (υ_{max}/cm^{-1}): 3062 (m, Ar. C-H), 2957 (s, Aliph. C-H), 1603 (m, Ar. -C = C), 1477 (m, Aliph. C-H), 1348 (w, Ar.–C-N), 1271 (s, -R-O-Ar). UV-Vis λ_{max} (nm) THF: 696, 334. Anal. Calc. For $C_{72}H_{64}CoN_8O_4$: C, 74.28; H, 5.54; Co, 5.06; N, 9.62; O, 5.50 Found: C, 73.66; H, 5.55; N, 9.76. MS (MALDI-TOF): *m/z* 1164.33 $[M + H]^+$.

Yield of **5**: 52 mg (49.7%). M.p. > 200 °C. FT-IR (υ_{max}/cm^{-1}): 3056 (m, Ar. C-H), 2960 (s, Aliph. C-H), 1607 (m, Ar. -C = C), 1486 (m, Aliph. C-H), 1350 (w, Ar.–C-N), 1228 (s, -R-O-Ar). UV-Vis λ_{max} (nm) THF: 700, 350, 320. Anal. Calc. For $C_{72}H_{64}CuN_8O_4$: C, 73.98; H, 5.52; Cu, 5.44; N, 9.59; O, 5.47 Found: C, 73.16; H, 5.39; N, 9.69. MS (MALDI-TOF): *m/z* 1168.72 $[M + H]^+$.

Yield of **6**: 31 mg (31.1%). M.p. > 200 °C. FT-IR (υ_{max}/cm^{-1}): 3060 (m, Ar. C-H), 2957 (s, Aliph. C-H), 1578 (m, Ar. -C = C), 1488 (m, Aliph. C-H), 1338 (w, Ar.–C-N), 1246 (s, -R-O-Ar). UV-Vis λ_{max} (nm) THF: 751, 523, 321. Anal. Calc. For $C_{72}H_{64}ClMnN_8O_4$: C, 72.32; H, 5.40; Cl, 2.96; Mn, 4.59; N, 9.37; O, 5.35 Found: C, 73.12; H, 5.23; N, 9.46. MS (MALDI-TOF): *m/z* 1160.86 $[M\text{-}Cl + H]^+$.

Biological investigation

Carbonic anhydrase and cholinesterase activities assays

The inhibitory efficacy of new complexes on BChE/AChE activities was obtained conforming to the spectrophotometric procedure of Ellman et al. (Bursal et al., 2019) and also performed according to our previous study (Huseynova et al., 2019). Briefly, red blood cells that were extracted from fresh blood were hemolyzed and the pH of the hemolysate obtained was modified at 4 °C to 8.7 with solid Tris (Ekinci et al., 2007). The Sepharose 4BL-tyrosine-sulfanilamide affinity column was coated with Human erythrocyte hemolysate. For 1.0 M NaCl/25 mM Na_2HPO_4 (pH 6.3) and 0.1 M $NaCH_3COO$/0.5 M $NaClO_4$ (pH 5.6), the human carbonic anhydrase isozymes (hCA I and hCA II) were eluted. Sodium dodecyl sulfate–polyacrylamide gel electrophoresis (SDS-PAGE) was applied and obtained in a single band for the purity of both isoenzymes. The protein determination in effluents showing activity was evaluated at 595 nm using the Bradford method spectrophotometrically (Bradford, 1976). Activities of CA isoenzymes were obtained following the Verpoorte et al. (1967) procedure. The spectrophotometric increase in the absorbance of the reaction medium was observed at 348 nm. The Lineweaver–Burk procedure (Lineweaver & Burk, 1934) CA activity (percent) versus inhibitory concentration was used to assess the inhibitory agents, and 1/V versus 1/[S] graphs were drawn. Bovine serum albumin has been used in detail as standard protein as previously given (Bayram et al., 2008; Burmaoğlu et al., 2016; Caglar et al., 2016). A percentage of activity versus inhibitor concentration graph was drawn for the designation of the inhibition efficacy of each phthalocyanine complexes with (4-isopropylbenzyl)oxy substituents on both hCA isoenzymes. Those graphs obtained the IC_{50} values. Three different novel concentrations of phthalocyanine complexes were used to calculate Ki values. In this study, graphs were given which are exhibited for the most effective inhibition of the studied compounds. The esterase activity determination method was used to determine these effects. According to this method, measurements were made every 5 min at a wavelength of 412 nm. Related graphs were created for the inhibition values of each molecule (%).

Molecular docking

Docking studies were performed against hCA I and II, cholinesterase enzymes for non-peripheral metallophthalocyanine complexes (**2–6**). As a result of the literature review, target proteins representing enzymes were procurement from the protein data bank. The 1BMZ target protein represents human carbonic anhydrase isoenzyme I, a major member of the metalloenzymes (Karthick & Tandon, 2016). 2ABE is a protein representing the L-histidine structure situated as the most abundant activator in human carbonic anhydrase isoenzyme II (Temperini et al., 2006). 4EY6 represents the catalytic anionic region to which the quaternary trimethylammonium choline moiety of ACh is attached and hydrolyzed at cholinergic chemical synapses in the central nervous system and the bottom of the binding site of the enzyme AChE found in neuromuscular junctions (da Costa et al., 2019; Malik et al., 2017). 2PM8 represents the N-terminal residue and toxic esters and an amino acid chain on the protein surface of butyrylcholine esterase, an enzyme involved in insulin resistance, which can hydrolyze many medical (Boyko et al., 2019). The molecular docking data were obtained by using the Development Company's Docking Server service and Virtua Drug research (Sayin et al., 2018).

Results

Synthesis and characterization

Figure 1 represents the synthetic route of novel soluble metallophthalocyanine complexes (**2–6**).

Phthalocyanine precursor (**1**) and its soluble zinc and indium phthalocyanines (**2** and **3**) were prepared according to the reported procedure (Güzel, Arslan, et al., 2019). Other targeted non-peripherally substituted phthalocyanines (**4–6**) were prepared by utilizing the anhydrous metal salts in DBU, the reaction colors turned dark green and the reaction was stopped. The reactions were continued using DBU and the anhydrous metal salts ($CoCl_2$ for **4**, $CuCl_2$ for **5** and $MnCl_3$ for **6**) and appropriate solvents (*n*-hexanol) at 165 °C. The crude complexes were obtained after washing several times with the alcohol/water mixture. The yields obtained for the cobalt, copper and manganese phthalocyanines (**4**, **5** and **6**) are 47%, 50% and 31%, respectively. Elucidation of the novel phthalocyanine complexes was performed with UV-Vis spectrophotometry, elemental analysis, FT-IR, ^{1}H-NMR spectroscopy and MALDI-TOF mass spectrometry. The FT-IR spectrum of phthalocyanines (**2–6**), the peak of the C≡N vibration of compound (**1**) at 2230 cm^{-1} disappeared as expected.

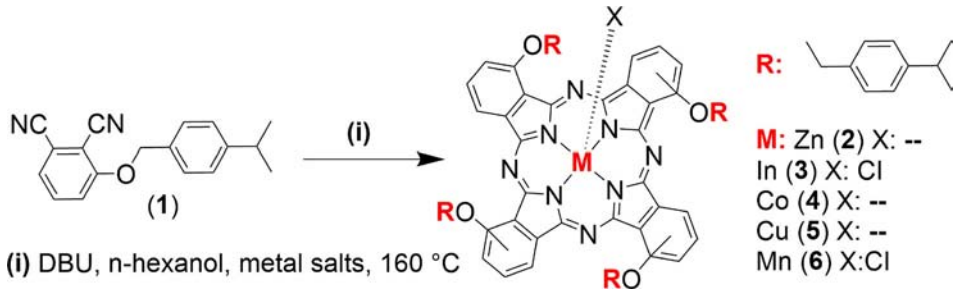

Figure 1. The synthesis of soluble metallophthalocyanine complexes (**2–6**).

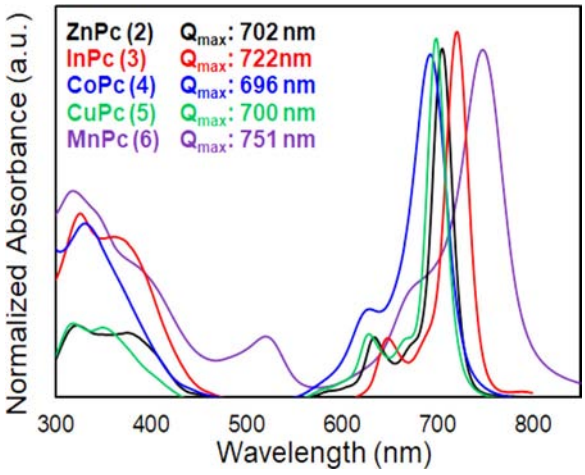

Figure 2. Normalized absorption spectra of the soluble non-peripherally substituted phthalocyanine complexes (**2–6**) in THF.

Stretching vibrations of aliphatic C-H bonds of phthalocyanines (**2–6**), as in the phthalonitrile derivative, were detected at around 2950 cm^{-1}. Similarly, stretching vibrations of aromatic C-H bonds of phthalocyanines (**2–6**) were observed at around 3050 cm^{-1}. ^{1}H-NMR investigations of phthalocyanine complexes **2** and **3** provided the expected chemical changes for the structure (Güzel, Orman, et al., 2019). ^{1}H-NMR spectra of (**4**, **5** and **6**) were precluded owing to their paramagnetic nature (Nas et al., 2017). The wide range of derivatives obtained by MALDI-TOF techniques confirmed the expected structures. Also, it has been found that the complexes synthesized in the structures observed without significant fragmentation are stable under MALDI-MS conditions. The molecular ion peaks were observed at *m/z*: 1169.75 $[M+H]^+$ for **2**, 1219.98 $[M\text{-}Cl+H]^+$ for **3**, 1164.33 $[M+H]^+$ for **4**, 1168.72 $[M+H]^+$ for **5** and 1160.86 $[M\text{-}Cl+H]^+$ for **6**.

Ground state electronic absorption spectra and aggregation behavior

Absorption spectroscopy is the first and most widely used method to determine the absorption properties of phthalocyanine complexes. These complexes show typical electronic spectra with two absorption regions. One of them is the UV region at about 300–350 nm (B band) and the other in the visible area at 600–700 nm (Q-band). UV-Vis spectra of the obtained phthalocyanines, the Q-bands, which are one of the characteristic bands for phthalocyanines and observed in the visible part, were seen at 702 nm for 2, 722 nm for 3, 696 nm for 4, 700 nm for 5 and 751 nm for 6 (Figure 2).

In metallophthalocyanine complexes (**2–6**), the single (narrow) Q-bands shown that these phthalocyanines are in monomeric form in the solvent medium. All complexes demonstrated intense single Q-absorption bands which are indicative of the metallophthalocyanines with the D4h symmetry. Also, indium and manganese phthalocyanine complexes (**3** and **6**) showed redshift when compared to other metallophthalocyanine complexes in this study. This could be explained by the fact that the larger indium atom is located out of the plane of the Pc cavity for complex **3**. The Q-band maximum of complex **6** shows a significant redshift concerning **2**, **4** and **5**, respectively, due to the oxidation state of Mn in the Pc ligand is +3, whereas Zn, Co and Cu are in oxidation state +2. Also, for manganese phthalocyanine complex (**6**) shows absorption at 524 nm, which was interpreted as a charge transfer absorption (phthalocyanine to metal, LMCT). Aggregation can often be explained as a very tight stacking of monomers, dimers and rings in the studied solvent. There are many factors in phthalocyanines that affect aggregation, such as concentration, nature of the solvent, peripheral and non-peripheral substituents, the metal ion in the macrocyclic nucleus and operating temperature (Atmaca et al., 2019; Güzel, Günsel, et al., 2017; Kurt et al., 2014).

To better observe the solubility and aggregation features of the phthalocyanines, dilution studies were carried out in THF solvent. As an illustrative example, non-peripherally substituted zinc phthalocyanine complex (**2**) was carried out using concentrations ranging from 2.5 μM to 20 μM (Figure 3).

Metabolic enzyme inhibition results

The hCA I and II isozymes are widely distributed throughout the body. CA I isoform is involved in cerebral and retinal edema, while CA II isoforms are involved in epilepsy and glaucoma. For example, inhibitory compounds that target hCA I are involved in cerebral and retinal edema, inhibitory compounds targeting hCA IV, II, XIV and XII as diuretics, in management edema, as drugs Antiepileptic, anticoagulant and also used for the treatment of some diseases. Carbonic anhydrase inhibitors (CAIs) have been developed to treat a variety of diseases since CA is involved in several important physiological functions such as lipogenesis, CO_2 and bicarbonate transfer, calcification, gluconeogenesis, tumorigenesis

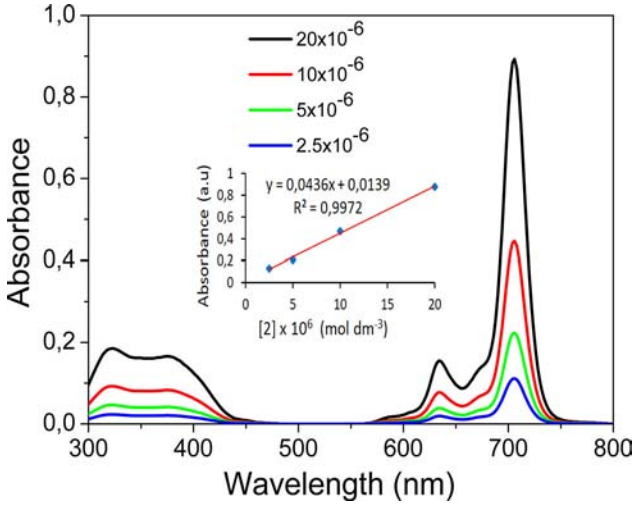

Figure 3. Electronic absorption spectra of **2** in THF at different concentrations. The inset shows the calibration plot for the Q-band maximum.

and bone resorption. Both hCA I and II isoenzymes, and also BChE and AChE were evaluated in this study. Enzymes results of this study:

1. For hCA I isoform, the Ki values were determined in the range of 478.13 ± 57.25–887.25 ± 101.20 μM. In comparison, the Ki for the standard CA inhibitor AZA (acetazolamide), a definitive hCA I inhibitor, was 851.53 ± 87.33 μmol/L against hCA I (Table 1). All metallophthalocyanine complexes (**2–6**) had effective inhibition effects than that of AZA. Also, between these compounds, manganese metallophthalocyanine complex (**6**), was the best hCA I inhibitor (Ki 478.13 ± 57.25 μM). As shown in Table 1, IC_{50} values are in the range of 412.46–903.74 μM toward hCA I, for hCA II are in the range of 481.04–945.88 μM. Metallophthalocyanine complexes (**2–6**) synthesized in this paper significantly inhibited hCA II with K_i in the low nanomolar range. K_i values were calculated between 525.16 ± 45.87 and 921.14 ± 81.25 μM (Table 1 and Figure 4). On the other hand, manganese metallophthalocyanine complex (**6**) (Ki: 525.16 ± 45.87 μM) is, in fact, the best inhibitor in these complexes, and also was better hCA II inhibitor compared to the clinical candidate drug (K_i of AZA: 1060.77 ± 98.0 μM).
2. AChE and BChE enzymes play an important role in the regulation of blood enzymes in the brain as important enzymes that differ in the kinetics, specificity of velocity and activity in several parts of brain cells. In the past decade, efforts to treat AD have focused on improving cholinergic neurotransmission in brain cells. This mechanism is largely based on the cholinergic hypothesis, which is evaluating cholinesterase enzyme inhibitors (ChEIs) that inhibit central cholinergic neurotransmission by inhibiting ACh degradation. In fact, ChEIs are currently the most promising treatment for AD because they reintroduce cholinergic function in human cells by increasing the amount of carbon in the central nervous system. As seen in Table 1, IC_{50} values are in the range of 87.63–284.92 μM toward AChE enzyme, for BChE enzyme, are in the range of 104.83–316.54 μM. In this work, AChE enzyme was also significantly inhibited by metallophthalocyanine complexes (**2–6**) at the low micromolar inhibition with K_i values in the range of 68.33 ± 9.13–201.15 ± 15.86 μM (Table 1). Indeed, the most powerful AChE inhibition was recorded by zinc phthalocyanine complex (**2**) with a K_i value of 68.33 ± 9.13 μM. Finally, metallophthalocyanine complexes (**2–6**) inhibited BChE with Ki values in the range of 86.25 ± 13.65–237.54 ± 24.7 μM (Table 1 and Figure 4). However, the most powerful BChE inhibition was obtained by zinc metallophthalocyanine (**2**) with a Ki value of 86.25 ± 13.65 μM.

Docking study

Docking studies were performed to investigate the inhibitory activity of newly synthesized metallophthalocyanine complexes (**2–6**) by central atom exchange against hCA I, hCA II, AChE and BChE enzymes. It was also detailed the secondary chemical interactions between the complexes studied with the amino acid residues of the target proteins. In docking studies, the estimated free energy of binding values of target proteins and metal complexes are given in Table 2.

The binding energies obtained from docking results for complexes and target proteins are given in Table 2. For a good physiological protein–ligand interaction, the binding energy should increase at negative values. The results show that the experimental IC_{50} values and the inhibition efficiencies determined by docking results are almost compatible. However, the predicted inhibition efficiency of complexes with the hCA I enzyme showed more affirmative results than the experimental IC_{50} values. This may be explained depending on the target protein structure selected. The selected target protein represents an active site of the enzyme. When the interactions between 1BMZ target protein and ZnPc (**2**) are examined, the oxygen atom formed a hydrogen bond with the nitrogen of GLN92. The oxygen, nitrogen and metal atom contain polar interaction with the Thr307 andGLU417 amino acid residues. The carbon atoms exhibit hydrophobic interactions with TRP5, PHE91, ALA121, LEU131, ALA135 and π–π interactions with TRP5, HIS67 and HIS200. In interactions of InPc (**3**) with 1BMZ, the oxygen and nitrogen atoms formed H-bonds with HIS64 and HIS67. Carbon atoms were performed hydrophobic interactions with ILE60, VAL62, ALA121, LEU141, VAL143, LEU198, TRP209 and π–π interactions with HIS64, HIS67, PHE91, HIS200, HIS119. As in the metal complexes with ZnPc (**2**) and InPc (**3**), the between the metal complex and 1BMZ target protein are present H-bond with GLN92, HIS96, THR199, polar interactions with GLN92, HIS94, hydrophobic interactions with HIS67, PHE91, ALA121, LEU131, PRO202, LEU198, VAL143, LEU141, LEU31, π–π interactions with HIS200, HIS94, PHE91. There are polar interactions with ASN69, hydrophobic interactions with PRO3, TRP5, VAL62, HIS67, PHE9, HIS94, ALA121, LEU131, PRO202 and π–π interactions with PHE91, HIS94 and HIS200 between the complex with Mn metal in MnPc (**6**) and 1BMZ without H-bonds. The absence of H-bonds from the

Table 1. The enzyme inhibition results of phthalocyanine complexes (**2–6**) against human carbonic anhydrase isoenzymes I and II (hCA I and II), acetylcholinesterase (AChE) and butyrylcholinesterase (BChE) enzymes.

	IC_{50} (μM)								K_i (μM)			
Compounds	hCA I	r^2	hCA II	r^2	AChE	r^2	BChE	r^2	hCA I	hCA II	AChE	BChE
ZnPc (**2**)	834.62	0.9727	883.62	0.9889	87.63	0.9582	104.83	0.9881	887.25 ± 101.20	905.42 ± 104.35	68.33 ± 9.13	86.25 ± 13.65
InPc (**3**)	632.04	0.9715	705.83	0.9526	284.92	0.9790	316.54	0.9733	668.37 ± 89.36	786.46 ± 143.54	201.15 ± 15.86	237.54 ± 24.7
CoPc (**4**)	903.74	0.9543	945.88	0.9830	105.94	0.9384	124.92	0.9824	856.14 ± 85.66	921.14 ± 81.25	78.21 ± 15.78	103.45 ± 10.13
CuPc (**5**)	506.24	0.9618	635.17	0.9783	114.85	0.9384	150.25	0.9518	588.13 ± 78.25	670.31 ± 90.36	98.36 ± 7.88	125.11 ± 10.05
MnPc (**6**)	412.46	0.9722	481.04	0.9598	168.37	0.9788	212.43	0.9711	478.13 ± 57.25	525.16 ± 45.87	125.24 ± 17.25	165.38 ± 23.84
AZA[a]	957.44	0.9350	964.78	0.9353	–	–	–	–	851.53 ± 87.33	1060.77 ± 98.0	–	–
TAC[b]	–	–	–	–	305.84	0.9631	383.80	0.9614	–	–	244.37 ± 25.47	290.25 ± 31.26

[a]Acetazolamide (AZA) was used as a control for hCA I and II.
[b]Tacrine (TAC) was used as a control for AChE and BChE enzymes.

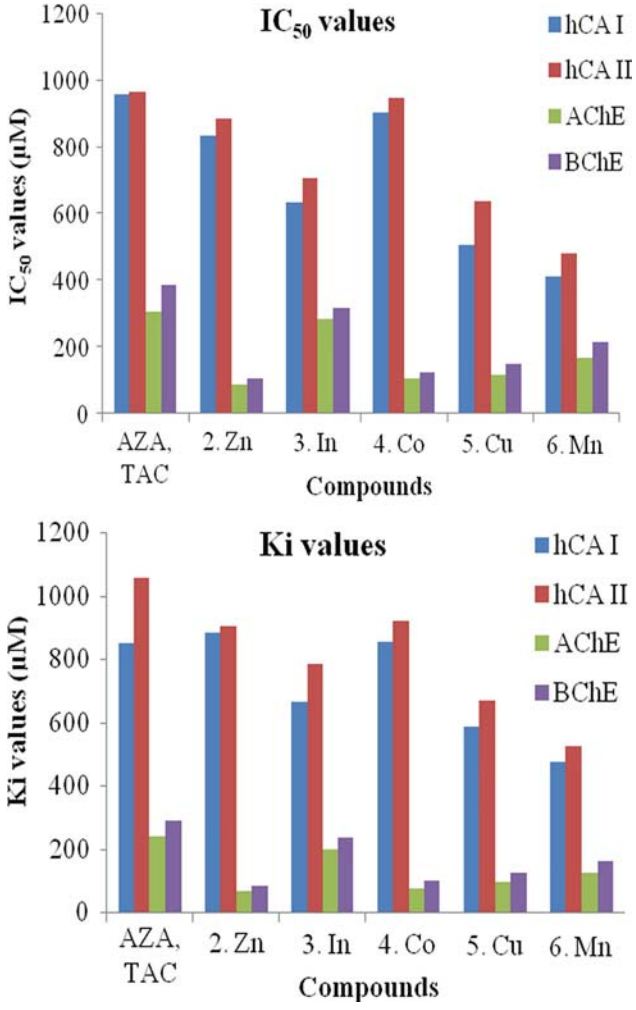

Figure 4. Comparative results of IC_{50} and Ki values of all compounds.

Table 2. The estimated free energy of binding (kcal/mol) between (**2–6**) complexes and the target protein.

	1BMZ	2ABE	4EY6	2PM8
ZnPc (**2**)	−3.61	−1.22	−6.04	−5.30
InPc (**3**)	−4.13	−1.57	−4.78	−4.27
CoPc (**4**)	−3.05	−1.24	−6.02	−5.25
CuPc (**5**)	−5.25	−2.12	−5.98	−5.18
MnPc (**6**)	−2.97	−4.28	−5.17	−5.02

secondary chemical interactions and the low number of interactions with amino acid residues proves why the binding energy is low. When the interactions of 2ABE target protein and ZnPc (**2**) were examined, nitrogen and oxygen atoms are made polar interactions with GLN92, HIS94, HIS96, HIS107, GLU117, HIS119, TRP209, HIS300, hydrophobic interactions with carbon atoms and PRO30, ALA65, VAL121, LEU141, VAL143, LEU198 and π–π interactions with HIS64, HIS94, HIS107, HIS109, TRP209, HIS300. The interactions of the InPc (**3**) are polar with GLN92, HIS94, GLU117, THR199, hydrophobic with PRO30, HIS64, ALA65, HIS119, VAL121, VAL121, VAL143, LEU198, VAL245 and π–π interactions with PHE131, TRP209, HIS300. The CuPc (**5**) as well as in the ZnPc (**2**) had polar interactions with HIS64, HIS119, HIS94, GLU106, HIS107, hydrophobic interactions with TYR7, PRO30, ALA65, VAL121, LEU198 and π–π interactions with HIS119, TRP209, HIS300 and HIS96. The complex with the highest interaction energy between 2ABE target protein and complexes is the MnPc (**6**). This phthalocyanine, unlike others, made H-bond with HIS64, THR200, GLU106, HIS96. Besides, the MnPc (**6**) is had hydrophobic interaction with ALA65 and cation–pi interaction with HIS94. The type and number of the interaction of complexes with 4EY6 and 2PM8 target proteins differ from the type and number of the interaction of other proteins. This may be due to the unsymmetrical molecular structures of proteins. Between 4EY6 and ZnPc (**2**), there is H-bond with SER347, ASP349 and hydrophobic interaction with LEU76. InPc (**3**) with the mentioned target protein exhibits polar interactions with SER347, ASP349, ASN350, hydrophobic with LEU76, TYR77, PRO344, LEU353, π–π interactions with TYR77. When the CoPc (**4**) is examined, it is seen that it makes H-bond with ASP349. Also, carbon atoms are in polar interaction with LEU79 and PRO344 and π–π interaction with TYR77. In the MnPc (**6**), the nitrogen atoms and the carbon atoms with ASP349 interact with H-bond and polar, respectively. Also, the carbon atoms are done hydrophobic and π–π interaction with PRO78 and TYR77, respectively. Finally, the H-bond between the ZnPc (**2**) with the 2PM8 target is formed with SER338 and polar interactions are performed with SER338 and ASN341. In the InPc (**3**), nitrogen, oxygen and indium metal only interact polarly with SER 388. In the CoPc (**4**) and CuPc (**5**) complexes, oxygen and nitrogen atoms formed H-bonds with SER338, respectively. Similarly, in these metals, carbon atoms exhibit hydrophobic interaction with ILE344 and PRO335, respectively. In the MnPc (**6**), nitrogen atom produced the polar interaction with SER338 amino acid residue and the hydrophobic interaction with the carbon atom and PRO335.

The molecular structures of the investigated complexes are similar. However, partial charges of the terminal atoms

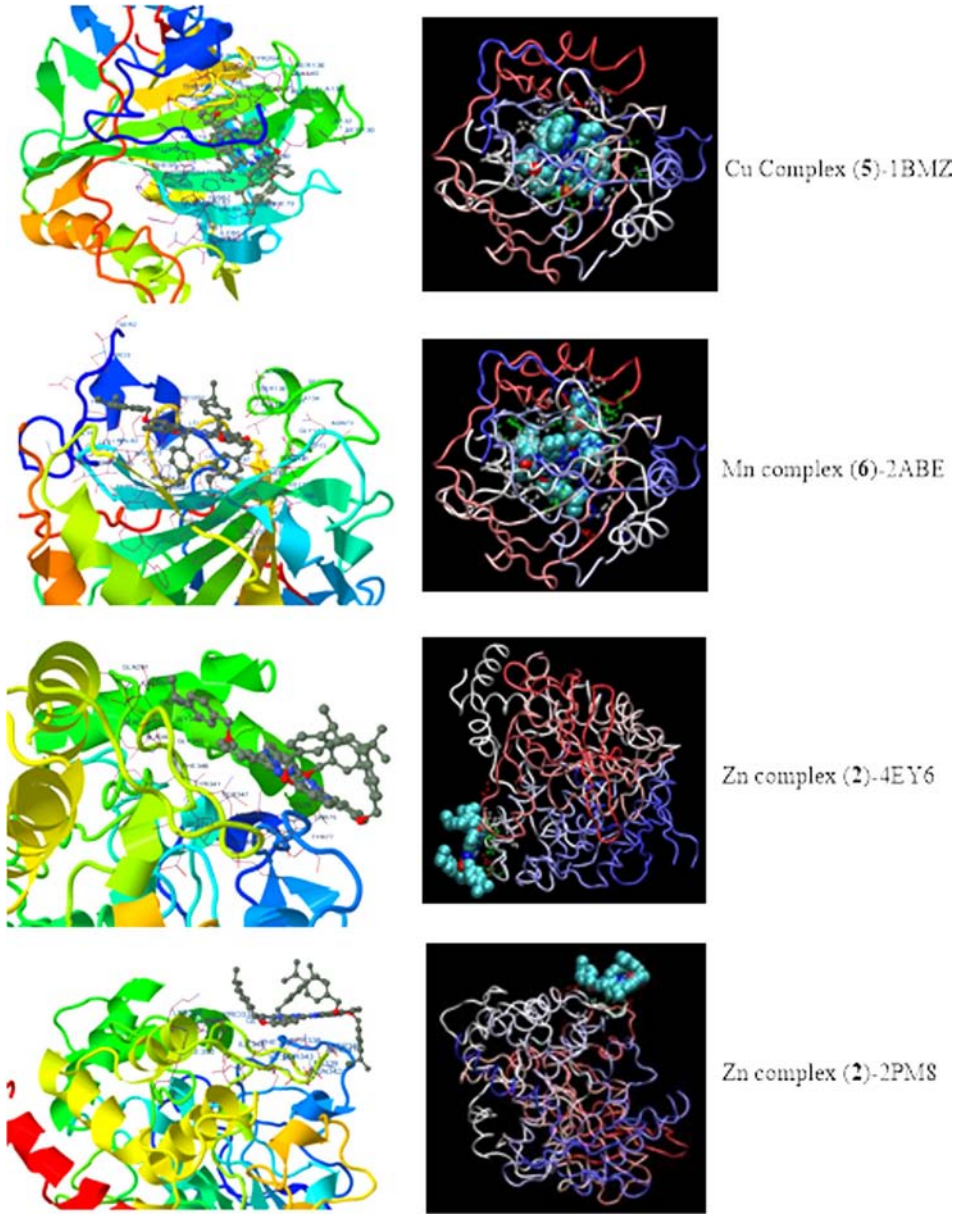

Figure 5. Docking pose of the most active inhibitor of each target protein.

vary depending on the gravitational force of the bond electrons of the central atom and exhibit different inhibitory activities and different secondary chemical interactions. Molecular simulation results can provide important information for the further development of enzyme inhibitors. While the interaction energy of CuPc (**5**) and MnPc (**6**) complexes with the 1BMZ and 2ABE target proteins was the highest, the interaction energy of 4EY6 and 2PM8 proteins with ZnPc (**2**) was the highest. According to the results given in Table 2, the mode of interaction with the most active inhibitor of each target protein is given in Figure 5.

Discussion

In this study, a series of new soluble metallophthalocyanine complexes synthesized and investigated enzyme inhibition properties. Synthesized complexes showed good inhibition effects against BChE, AChE, hCA I and hCA II enzymes. Especially, zinc and manganese metallophthalocyanine complexes (**2** and **6**) can be good candidate drugs, the same as AChE, BChE and CA inhibitor complexes, respectively. In this manner, these novel complexes can use for therapy of some diseases like epilepsy, mountain sickness, AD, gastric and duodenal ulcers, glaucoma, osteoporosis or neurological disorders. The binding interaction of these active compounds with hCA isoenzymes I and II (hCA I and II), AChE and BChE enzymes was supported in detail using molecular insertion.

Author contributions

Specific author contributions are as follow: Designing the study: Emre Güzel, Ümit M. Koçyiğit, Parham Taslimi, İlhami Gülçin; Collecting and analyzing the data: Emre Güzel, Ümit M. Koçyiğit; Drafting the manuscript: Emre Güzel, Ümit M. Koçyiğit; Visualization and revising: İlkay Şişman, Mehmet

Nebioğlu, Barış S. Arslan, Emre Güzel; Theoretical calculations: Sultan Erkan; Supervision: Emre Güzel, Ümit M. Koçyiğit.

Disclosure statement

The authors declare that there is no conflict of interest.

Funding

This work was supported by the Research Fund of the Sakarya University (Project No: 2019-5-19-174) and Sakarya University of Applied Sciences.

ORCID

Emre Güzel https://orcid.org/0000-0002-1142-3936
Ümit M. Koçyiğit https://orcid.org/0000-0001-8710-2912
Parham Taslimi http://orcid.org/0000-0002-3171-0633
İlhami Gülçin https://orcid.org/0000-0001-5993-1668
Sultan Erkan https://orcid.org/0000-0001-6744-929X

References

Atilla, D., Durmuş, M., Gürek, A. G., Ahsen, V., & Nyokong, T. (2007). Synthesis, photophysical and photochemical properties of poly(oxyethylene)-substituted zinc phthalocyanines. *Dalton Transactions*, *12*(12), 1235–1243. https://doi.org/10.1039/B617773E

Atmaca, G. Y., Yakan, H., Kutuk, H., Nebioğlu, M., Güzel, E., & Erdoğmuş, A. (2019). Phthalocyanines with bromobenzenesulfanyl substituents at non-peripheral position: Preparation, photophysical and photochemical properties. *Journal of Porphyrins and Phthalocyanines*, *23*(7–8), 821–827. https://doi.org/10.1142/S1088424619500676

Bayram, E., Senturk, M., Irfan Kufrevioglu, O., & Supuran, C. T. (2008). *In vitro* inhibition of salicylic acid derivatives on human cytosolic carbonic anhydrase isozymes I and II. *Bioorganic & Medicinal Chemistry*, *16*(20), 9101–9105. https://doi.org/10.1016/j.bmc.2008.09.028

Boyko, K. M., Baymukhametov, T. N., Chesnokov, Y. M., Hons, M., Lushchekina, S. V., Konarev, P. V., Lipkin, A. V., Vasiliev, A. L., Masson, P., Popov, V. O., & Kovalchuk, M. V. (2019). 3D structure of the natural tetrameric form of human butyrylcholinesterase as revealed by cryoEM, SAXS and MD. *Biochimie*, *156*, 196–205. https://doi.org/10.1016/j.biochi.2018.10.017

Boztas, M., Taslimi, P., Yavari, M. A., Gulcin, I., Sahin, E., & Menzek, A. (2019). Synthesis and biological evaluation of bromophenol derivatives with cyclopropyl moiety: Ring opening of cyclopropane with monoester. *Bioorganic Chemistry*, *89*, 103017. https://doi.org/10.1016/j.bioorg.2019.103017

Bradford, M. M. (1976). A rapid and sensitive method for the quantitation of microgram quantities of protein utilizing the principle of protein-dye binding. *Analytical Biochemistry*, *72*, 248–254. https://doi.org/10.1016/0003-2697(76)90527-3

Burmaoğlu, S., Dilek, E., Yılmaz, A. O., & Supuran, C. T. (2016). Synthesis of two phloroglucinol derivatives with cinnamyl moieties as inhibitors of the carbonic anhydrase isozymes I and II: An *in vitro* study. *Journal of Enzyme Inhibition and Medicinal Chemistry*, *31*(sup2), 208–212. https://doi.org/10.1080/14756366.2016.1181626

Bursal, E., Aras, A., Kılıç, Ö., Taslimi, P., Gören, A. C., & Gülçin, İ. (2019). Phytochemical content, antioxidant activity, and enzyme inhibition effect of *Salvia eriophora* Boiss. & Kotschy against acetylcholinesterase, α-amylase, butyrylcholinesterase, and α-glycosidase enzymes. *Journal of Food Biochemistry*, *43*(3), e12776. https://doi.org/10.1111/jfbc.12776

Caglar, S., Dilek, E., Caglar, B., Adiguzel, E., Temel, E., Buyukgungor, O., & Tabak, A. (2016). New metal complexes with diclofenac containing 2-pyridineethanol or 2-pyridinepropanol: Synthesis, structural, spectroscopic, thermal properties, catechol oxidase and carbonic anhydrase activities. Journal *of Coordination Chemistry*, *69*(22), 3321–3335. https://doi.org/10.1080/00958972.2016.1227802

Chino, Y., Ohta, K., Kimura, M., & Yasutake, M. (2017). Discotic liquid crystals of transition metal complexes: Synthesis and mesomorphism of phthalocyanines substituted by m-alkoxyphenylthio groups. *Journal of Porphyrins and Phthalocyanines*, *21*(3), 159–178. https://doi.org/10.1142/S1088424617500389

Çimen, Y., Ermiş, E., Dumludağ, F., Özkaya, A. R., Salih, B., & Bekaroğlu, Ö. (2014). Synthesis, characterization, electrochemistry and VOC sensing properties of novel ball-type dinuclear metallophthalocyanines. *Sensors and Actuators B: Chemical*, *202*, 1137–1147. https://doi.org/10.1016/j.snb.2014.06.066

da Costa, G. V., Ferreira, E. F. B., da S. Ramos, R., da Silva, L. B., de Sá, E. M. F., da Silva, A. K. P., Lobato, C. M., Souto, R. N. P., T. de P. da Silva, C. H., Federico, L. B., Rosa, J. M. C., & dos Santos, C. B. R. (2019). Hierarchical virtual screening of potential insectides inhibitors of acetylcholinesterase and juvenile hormone from temephos. *Pharmaceuticals*, *12*(2), 61. https://doi.org/10.3390/ph12020061

Ekinci, D., Beydemir, Ş., & Küfrevİoğlu, Ö. İ. (2007). *In vitro* inhibitory effects of some heavy metals on human erythrocyte carbonic anhydrases. *Journal of Enzyme Inhibition and Medicinal Chemistry*, *22*(6), 745–750. https://doi.org/10.1080/14756360601176048

El-Sayed, N. A. E., Farag, A. E. S., Ezzat, M. A. F., Akincioglu, H., Gülçin, İ., & Abou-Seri, S. M. (2019). Design, synthesis, in vitro and in vivo evaluation of novel pyrrolizine-based compounds with potential activity as cholinesterase inhibitors and anti-Alzheimer's agents. *Bioorganic Chemistry*, *93*, 103312. https://doi.org/10.1016/j.bioorg.2019.103312

Erdemir, F., Celepci, D. B., Aktaş, A., Gök, Y., Kaya, R., Taslimi, P., Demir, Y., & Gulçin, İ. (2019). Novel 2-aminopyridine liganded Pd(II) N-heterocyclic carbene complexes: Synthesis, characterization, crystal structure and bioactivity properties. *Bioorganic Chemistry*, *91*, 103134. https://doi.org/10.1016/j.bioorg.2019.103134

Genç Bilgiçli, H., Kestane, A., Taslimi, P., Karabay, O., Bytyqi-Damoni, A., Zengin, M., & Gulçin, İ. (2019). Novel eugenol bearing oxypropanolamines: Synthesis, characterization, antibacterial, antidiabetic, and anticholinergic potentials. *Bioorganic Chemistry*, *88*, 102931. https://doi.org/10.1016/j.bioorg.2019.102931

Gürek, A. G., & Bekaroğlu, Ö. (1994). Octakis(alkylthio)-substituted phthalocyanines and their interactions with silver(I) and palladium(II) ions. *Journal of the Chemical Society, Dalton Transactions*, *9*, 1419–1423. https://doi.org/10.1039/DT9940001419

Güzel, E. (2019). Dual-purpose zinc and silicon complexes of 1,2,3-triazole group substituted phthalocyanine photosensitizers: Synthesis and evaluation of photophysical, singlet oxygen generation, electrochemical and photovoltaic properties. *RSC Advances*, *9*(19), 10854–10864. https://doi.org/10.1039/C8RA10665G

Güzel, E., Arslan, B. S., Atmaca, G. Y., Nebioğlu, M., & Erdoğmuş, A. (2019). High photosensitized singlet oxygen generating zinc and chloroindium phthalocyanines bearing (4-isopropylbenzyl)oxy groups as potential agents for photophysicochemical applications. *ChemistrySelect*, *4*(2), 515–520. https://doi.org/10.1002/slct.201803255

Güzel, E., Atmaca, G. Y., Erdoğmuş, A., & Koçak, M. B. (2017). Novel sulfonated hydrophilic indium(III) and gallium(III) phthalocyanine photosensitizers: Preparation and investigation of photophysicochemical properties. *Journal of Coordination Chemistry*, *70*(15), 2659–2670. https://doi.org/10.1080/00958972.2017.1366471

Güzel, E., Atsay, A., Nalbantoglu, S., Şaki, N., Dogan, A. L., Gül, A., & Koçak, M. B. (2013). Synthesis, characterization and photodynamic activity of a new amphiphilic zinc phthalocyanine. *Dyes and Pigments*, *97*(1), 238–243. https://doi.org/10.1016/j.dyepig.2012.12.027

Güzel, E., Günsel, A., Bilgiçli, A. T., Atmaca, G. Y., Erdoğmuş, A., & Yarasir, M. N. (2017). Synthesis and photophysicochemical properties of novel thiadiazole-substituted zinc (II), gallium (III) and silicon (IV) phthalocyanines for photodynamic therapy. *Inorganica Chimica Acta*, *467*, 169–176. https://doi.org/10.1016/j.ica.2017.07.058

Güzel, E., Orman, E. B., Köksoy, B., Çelikbıçak, Ö., Bulut, M., & Özkaya, A. R. (2019). Comparative electrochemistry and electrochromic application of novel binuclear double-decker rare earth metal phthalocyanines bearing 4-(hydroxyethyl)phenoxy moieties. *Journal of the*

Electrochemical Society, *166*(10), H438–H451. https://doi.org/10.1149/2.0511910jes

Huseynova, M., Medjidov, A., Taslimi, P., & Aliyeva, M. (2019). Synthesis, characterization, crystal structure of the coordination polymer Zn(II) with thiosemicarbazone of glyoxalic acid and their inhibitory properties against some metabolic enzymes. *Bioorganic Chemistry*, *83*, 55–62. https://doi.org/10.1016/j.bioorg.2018.10.012

Karthick, T., & Tandon, P. (2016). Computational approaches to find the active binding sites of biological targets against busulfan. *Journal of Molecular Modeling*, *22*(6), 142. https://doi.org/10.1007/s00894-016-3015-z

Korkut, S. E., Ocak, H., Bilgin-Eran, B., Güzeller, D., & Şener, M. K. (2017). Lyotropic liquid crystalline phthalocyanines containing 4-((S)-3,7-dimethyloctyloxy)phenoxy moieties. *Journal of Porphyrins and Phthalocyanines*, *21*(1), 16–23. https://doi.org/10.1142/S1088424616501261

Kurt, Ö., Özçeşmeci, I., Gül, A., & Koçak, M. B. (2014). Synthesis and photophysical properties of novel hexadeca-substituted phthalocyanines bearing three different groups. *Journal of Organometallic Chemistry*, *754*, 8–15. https://doi.org/10.1016/j.jorganchem.2013.12.044

Lineweaver, H., & Burk, D. (1934). The determination of enzyme dissociation constants. *Journal of the American Chemical Society*, *56*(3), 658–666. https://doi.org/10.1021/ja01318a036

Malik, R., Choudhary, B. S., Srivastava, S., Mehta, P., & Sharma, M. (2017). Identification of novel acetylcholinesterase inhibitors through e-pharmacophore-based virtual screening and molecular dynamics simulations. *Journal of Biomolecular Structure and Dynamics*, *35*(15), 3268–3284. https://doi.org/10.1080/07391102.2016.1253503

Mamedova, G., Mahmudova, A., Mamedov, S., Erden, Y., Taslimi, P., Tüzün, B., Tas, R., Farzaliyev, V., Sujayev, A., Alwasel, S. H., & Gulçin, İ. (2019). Novel tribenzylaminobenzolsulphonylimine based on their pyrazine and pyridazines: Synthesis, characterization, antidiabetic, anticancer, anticholinergic, and molecular docking studies. *Bioorganic Chemistry*, *93*, 103313. https://doi.org/10.1016/j.bioorg.2019.103313

Nas, A., Biyiklioglu, Z., Fandaklı, S., Sarkı, G., Yalazan, H., & Kantekin, H. (2017). Tetra(3-(1,5-diphenyl-4,5-dihydro-1H-pyrazol-3-yl)phenoxy) substituted cobalt, iron and manganese phthalocyanines: Synthesis and electrochemical analysis. *Inorganica Chimica Acta*, *466*, 86–92. https://doi.org/10.1016/j.ica.2017.05.050

Önal, E., Okyay, T. M., Ekineker, G., İşci, Ü., Ahsen, V., Berber, S., Zorlu, Y., & Dumoulin, F. (2018). Sulfanyl vs sulfonyl, 4,5- vs 3,6-position. How structural variations in phthalonitrile substitution affect their infra-red, crystallographic and Hirshfeld surface analyses. *Journal of Molecular Structure*, *1155*, 310–319. https://doi.org/10.1016/j.molstruc.2017.10.069

Ozoemena, K., & Nyokong, T. (2002). Octabutylthiophthalocyaninatoiron(II): Electrochemical properties and interaction with cyanide. *Journal of the Chemical Society, Dalton Transactions*, *8*, 1806–1811. https://doi.org/10.1039/b111429h

Sayin, K., Karakaş, D., Kariper, S. E., & Sayin, T. A. (2018). Computational study of some fluoroquinolones: Structural, spectral and docking investigations. *Journal of Molecular Structure*, *1156*, 172–181. https://doi.org/10.1016/j.molstruc.2017.11.091

Sobotta, L., Lijewski, S., Dlugaszewska, J., Nowicka, J., Mielcarek, J., & Goslinski, T. (2019). Photodynamic inactivation of *Enterococcus faecalis* by conjugates of zinc(II) phthalocyanines with thymol and carvacrol loaded into lipid vesicles. *Inorganica Chimica Acta*, *489*, 180–190. https://doi.org/10.1016/j.ica.2019.02.031

Taslimi, P., Türkan, F., Cetin, A., Burhan, H., Karaman, M., Bildirici, I., Gulçin, İ., & Şen, F. (2019). Pyrazole[3,4-d]pyridazine derivatives: Molecular docking and explore of acetylcholinesterase and carbonic anhydrase enzymes inhibitors as anticholinergics potentials. *Bioorganic Chemistry*, *92*, 103213. https://doi.org/10.1016/j.bioorg.2019.103213

Temperini, C., Scozzafava, A., & Supuran, C. T. (2006). Carbonic anhydrase activators: The first X-ray crystallographic study of an adduct of isoform I. *Bioorganic & Medicinal Chemistry Letters*, *16*(19), 5152–5156. https://doi.org/10.1016/j.bmcl.2006.07.021

Turkan, F., Cetin, A., Taslimi, P., Karaman, H. S., & Gulçin, İ. (2019a). Synthesis, characterization, molecular docking and biological activities of novel pyrazoline derivatives. *Archiv der Pharmazie*, *352*(6), 1800359. https://doi.org/10.1002/ardp.201800359

Turkan, F., Cetin, A., Taslimi, P., Karaman, M., & Gulçin, İ. (2019b). Synthesis, biological evaluation and molecular docking of novel pyrazole derivatives as potent carbonic anhydrase and acetylcholinesterase inhibitors. *Bioorganic Chemistry*, *86*, 420–427. https://doi.org/10.1016/j.bioorg.2019.02.013

van de Winckel, E., David, B., Simoni, M. M., González-Delgado, J. A., de la Escosura, A., Cunha, Â., & Torres, T. (2017). Octacationic and axially di-substituted silicon (IV) phthalocyanines for photodynamic inactivation of bacteria. *Dyes and Pigments*, *145*, 239–245. https://doi.org/10.1016/j.dyepig.2017.06.004

Verpoorte, J. A., Mehta, S., & Edsall, J. T. (1967). Esterase activities of human carbonic anhydrases B and C. *Journal of Biological Chemistry*, *242*, 4221–4229.

Wierzchowski, M., Łażewski, D., Tardowski, T., Grochocka, M., Czajkowski, R., Sobiak, S., & Sobotta, L. (2020). Nanomolar photodynamic activity of porphyrins bearing 1,4,7-trioxanonyl and 2-methyl-5-nitroimidazole moieties against cancer cells. *Journal of Photochemistry and Photobiology B: Biology*, *202*, 111703. https://doi.org/10.1016/j.jphotobiol.2019.111703

Yıldız, B., Güzel, E., Akyüz, D., Arslan, B. S., Koca, A., & Şener, M. K. (2019). Unsymmetrically pyrazole-3-carboxylic acid substituted phthalocyanine-based photoanodes for use in water splitting photoelectrochemical and dye-sensitized solar cells. *Solar Energy*, *191*, 654–662. https://doi.org/10.1016/j.solener.2019.09.043